Experimental evidence of anomalous phase synchronization in two diffusively coupled Chua oscillators

Syamal Kumar Dana[a)]
Instrument Division, Indian Institute of Chemical Biology, Jadavpur, Kolkata 700032, India

Bernd Blasius[b)] and Jürgen Kurths[c)]
Institut für Physik, Universität Potsdam, Postfach 601553, D-14415, Germany

(Received 1 October 2005; accepted 28 March 2006; published online 11 May 2006)

We study the transition to phase synchronization in two diffusively coupled, nonidentical Chua oscillators. In the experiments, depending on the used parameterization, we observe several distinct routes to phase synchronization, including states of either in-phase, out-of-phase, or antiphase synchronization, which may be intersected by an intermediate desynchronization regime with large fluctuations of the frequency difference. Furthermore, we report the first experimental evidence of an anomalous transition to phase synchronization, which is characterized by an initial enlargement of the natural frequency difference with coupling strength. This results in a maximal frequency disorder at intermediate coupling levels, whereas usual phase synchronization via monotonic decrease in frequency difference sets in only for larger coupling values. All experimental results are supported by numerical simulations of two coupled Chua models. © *2006 American Institute of Physics*. [DOI: 10.1063/1.2197168]

The collective behavior of coupled nonlinear oscillators is of significant interest in many areas of science and technology. Synchronization appears as one of the most fundamental phenomena in such systems, where the interaction is able to attune the motion among the oscillators. It has been shown that several forms of synchronization can be displayed even in chaotic systems. Of special importance is the notion of phase synchronization in nonidentical oscillators, where coupling is able to overcome the parameter mismatch and the oscillators mutually adjust their frequencies to a common synchronized frequency, while the phases become locked. Usually the introduction of coupling simply promotes the existence of such coherent oscillations among the oscillators. However in nonlinear systems the response of the system to the onset of coupling may be quite different. In the so-called anomalous route to phase synchronization, with the addition of weak coupling, the frequency difference between two oscillators can be even larger. Furthermore, here we show that depending on the system parameters, different synchronization states, such as in-phase or antiphase, can be initiated. Despite these interesting results very few experiments have been done to explore the full complexity of the issue. Here we present the first experimental verification of these effects in chaotic oscillating electronic circuits.

I. INTRODUCTION

Synchronization among interacting nonlinear oscillators is one the most fundamental problems in nonlinear dynamics with application in many areas of science and technology.[1–4] Synchronization is a ubiquitous phenomenon and in the course of time different forms of synchronization have been identified. Most notably, two identical chaotic oscillators can attain a state of complete synchronization, in which the motion takes place on an invariant synchronization manifold.[5] In the case of generalized synchronization the instantaneous states of the subsystems are interrelated by a functional dependence.[6] In contrast, the notion of phase synchronization (PS) refers to a weaker form of synchrony between chaotic systems, where two or many interacting oscillators with varying natural frequencies develop a perfect phase locking relation for weak coupling, although the amplitudes may remain almost uncorrelated.[7–9] For interaction strength above a critical value the coupled oscillators then rotate with a common frequency. PS is abundant in science and it is found to play a crucial role in many weakly interacting natural systems,[3] in lasers,[10] and also in electronic circuits.[11] The presence of PS has been confirmed in many living systems, including the cardio-respiratory rhythm,[12] neural oscillator,[13] as well as behavioral psychology[14] or ecology.[15]

Usually one would assume that increasing the interaction between the oscillators could only enhance the amount of synchronization. However, in nonlinear systems the onset of coupling may also give rise to unexpected behaviors such as oscillation death[16] or dephasing with bursts of amplitude change.[17] In two identical chaotic systems coupling may destabilize[18] the state of complete synchronization in a short-wavelength bifurcation, where the synchronous state becomes unstable at a critical coupling strength due to a zero crossing of the largest transverse Lyapunov exponent. Other counterintuitive effects of coupling can appear if the oscillators are nonidentical and differ in their natural frequency of oscillation. In this case the usual route to phase synchroniza-

[a)]Electronic mail: skdana@iicb.res.in
[b)]Electronic mail: bernd@agnld.uni-potsdam.de
[c)]Electronic mail: juergen@agnld.uni-potsdam.de

tion (PS) predicts that the frequency difference should, in general, decrease monotonically with coupling strength and disappear above a critical value.[3] Recently, a marked departure[19] from this common notion has been observed in a foodweb model.[15] Contrary to expectation, a large population of nonidentical oscillators shows an initial amplification of the frequency disorder with coupling, which is followed by the usual monotonic decrease in frequency disorder only for further increase in coupling strength. Such an unusual enlargement of the frequency disorder in the weaker coupling range with a maximal value of the frequency disorder at intermediate coupling range has been denoted as *anomalous phase synchronization* (APS).[19–21] The anomalous transition effectively results in an inhibition of PS, since a larger coupling strength is necessary for inducing phase locking, compared to the usual route to PS. However, for an appropriate choice of the system parameters, the onset of PS may also be enhanced,[19] i.e., phase locking may be achieved for coupling smaller than what is usually required to establish PS.

It has been shown[19] that APS originates in the nonisochronicity of oscillation and arises when the nonisochronicity covaries with the natural frequency of the oscillation. Nonisochronicity as a shear of phase flow[22] induces an amplitude dependence of the natural frequency of an oscillator. Due to their mutual interaction the oscillators are perturbed off their free limit cycle, which as a consequence may detune the oscillators in such a way that their natural frequency difference is enlarged. On the other hand, synchronization can also be enhanced by this mechanism when nonisochronicity and natural frequency have negative covariance. As a consequence, APS is characterized by a smooth increase of the frequency difference with the coupling strength and sets in without threshold. It is in this way distinguished from other types of coupling-induced desynchronization bifurcations (e.g., short-wavelength bifurcation), where the synchronization state is destabilized at a critical coupling strength.[18]

APS is established as a universal phenomenon and it has been observed in a large number of different model systems and also for various coupling types, e.g., with local and global coupling.[19] The exact condition for APS in any coupled system can be derived when two or more parameters of a system are functionally dependent.[19] For example, contrary to previous results,[3] APS can also be found in coupled Rössler oscillators by an appropriate selection of the system parameters.[19] APS appears already in only two interacting oscillators and it is robust to, and can even be enhanced by, the presence of noise.[20] Recently, by numerical simulations in two interacting Ginzburg-Landau systems, it has been shown that APS can also arise in spatially extended systems.[21] However, up to now any experimental verification of APS is still eluding the researchers.

In this paper we report the first experimental evidence of APS in two diffusively coupled Chua oscillators. In our experiments, we measure the frequency difference $\Delta\Omega$ and the evolution of the phase difference $\Delta\phi(t)$ in two diffusively coupled Chua oscillators as a function of the interaction strength between the two circuits. The experimental results are compared with direct numerical simulations. As our main result, we find clear evidence for the presence of anomalous synchronization transitions in coupled Chua circuits, both in our experiments and in the numerical simulations. Furthermore, in contrast to previous studies, the onset of phase synchronization in our system turned out to be rather involved. Depending on the sign and the magnitude of the frequency mismatch between the two oscillators, we observe very different—and so far not described—routes to phase synchronization, involving successive transitions between different synchronization states (e.g., in-phase or antiphase) and various forms of APS.

If the frequency mismatch between the two oscillators is adjusted to be comparatively large, we observe an anomalous route to a state of *in-phase synchronization*, which is characterized by a small absolute value of the locked phase difference ($|\Delta\phi| \ll$ constant). In contrast, for a smaller natural frequency mismatch we observe an enhanced transition to antiphase synchronization ($|\Delta\phi| \approx \pi$) at much weaker coupling. To be more precise, for increasing the coupling strength from zero above a first coupling threshold the two oscillators are synchronized in a state of *out-of-phase synchronization*, characterized by a large value of the phase difference ($0 < |\Delta\phi| < \pi$). With increasing coupling the, still bounded, phase difference attains larger values, which eventually leads to a state of *antiphase synchronization* ($|\Delta\phi| \approx \pi$), immediately before the transition to a large desynchronization regime. Finally, above a second critical coupling strength, the desynchronization disappears and the oscillators tune into a state of in-phase synchrony. Beside these two synchronization transitions, we observe another route to phase synchronization, which is realized by reversing the sign of the frequency mismatch (a fact which emphasizes the effective role played by coupling asymmetry for the anomalous transition to PS). In this case, we first observe an anomalous transition to antiphase synchronization, which is again followed by a large desynchronization regime and then a second regime of phase synchronization.

One common property of these different synchronization routes is the presence of several distinct synchronized states (in-phase, out-of-phase, and antiphase), which are separated by an intermediate desynchronization regime. Similar transitions have been reported in a few recent studies to appear in a neural model,[23] in delay-coupled phase oscillators[24] and in a model of recurrent epidemics.[25] We would like to stress that these synchronization routes and also states of antiphase synchronization, to our knowledge, have never before been observed or discussed in connection with APS.[19] Furthermore, experimental evidence of such a transition from antiphase to in-phase via a desynchronization regime has not been reported earlier.

The paper is structured as follows: In Sec. II we describe our experimental setup of two diffusively coupled Chua circuits and also the model, which is used for the numerical simulations. In Sec. III we consecutively describe three different experiments, which demonstrate the typical routes to phase synchronization, which are exhibited in our system. Finally, our findings are summarized in the Conclusion.

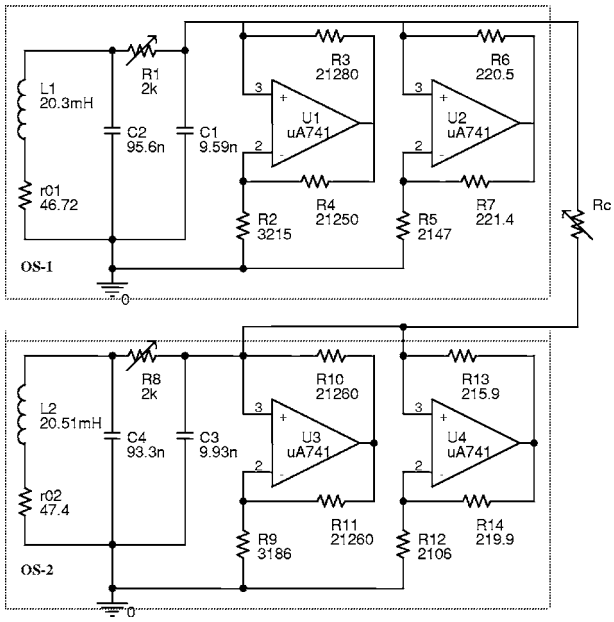

FIG. 1. Two coupled Chua oscillators: Power supply is ±9 V. The oscillators are identified as OS-1 and OS-2 within the dotted boxes. The component values are shown below each symbol. Unit of resistance is in Ohm, the capacitor is in Faraday.

II. EXPERIMENTAL SETUP: TWO DIFFUSIVELY COUPLED CHUA OSCILLATORS

In this work we study both experimentally and numerically the synchronization arising in two diffusively coupled nonidentical Chua oscillators as shown in Fig. 1. Each oscillator consists of linear passive elements as a resistor $R_{1,8}$, inductor $L_{1,2}$, capacitors $C_{1,3}$, $C_{2,4}$, and one nonlinear resistance. In our notation, here, the first or second index always denotes the respective element of the first or second oscillator (see Fig. 1 and Table I). The nonlinear resistance is approximated by a piecewise linear function and in our experiments it is designed by a pair of linear amplifiers (U1-U2 or U3-U4: μA741) for each oscillator. The resistance R_C determines the coupling strength $\epsilon=1/R_C$.

The model of the two diffusively coupled Chua oscillators, in dimensionless form, is given by

$$\frac{dx_1}{d\tau} = \alpha_1[(y_1 - x_1) - f(x_1)] + \epsilon_1\alpha_1(x_2 - x_1),$$

$$\frac{dy_1}{d\tau} = (x_1 - y_1 + z_1),$$

$$\frac{dz_1}{d\tau} = -\beta_1 y_1 - \gamma_1 z_1,$$

$$\frac{dx_2}{d\tau} = \tau_c\alpha_2[(y_2 - x_2) - f(x_2)] + \epsilon_2\alpha_2\tau_c(x_1 - x_2),$$

$$\frac{dy_2}{d\tau} = \tau_c(x_2 - y_2 + z_2),$$

$$\frac{dz_2}{d\tau} = \tau_c(-\beta_2 y_2 - \gamma_2 z_2), \tag{1}$$

where the piecewise linear function $f(x_{1,2})$ is defined as

$$f(x_{1,2}) = \begin{cases} b_{1,2}x_{1,2} + (b_{1,2} - a_{1,2}) & \text{if } x_{1,2} < -1 \\ a_{1,2}x_{1,2} & \text{if } -1 \leqslant x_{1,2} \leqslant 1 \\ b_{1,2}x_{1,2} + (a_{1,2} - b_{1,2}) & \text{if } x_{1,2} > 1 \end{cases} \tag{2}$$

and $\tau=t/R_1C_2$, $\tau_c=R_1C_2/R_8C_4$ and $\alpha_1=C_2/C_1$, $\beta_1=R_1^2C_2/L_1$, $\gamma_1=R_1r_{01}C_2/L_1$, $\alpha_2=C_4/C_3$, $\beta_2=R_8^2C_4/L_2$, $\gamma_2=R_8r_{02}C_4/L_2$, $\epsilon_1=\epsilon R_1$, $\epsilon_2=\epsilon R_8$ and $\epsilon=1/R_C$. The state variables are the dimensionless voltages $x_{1,2}=V_{C1,C3}/E$, $y_{1,2}=V_{C2,C4}/E$ at the respective capacitor nodes and $z_{1,2}=R_{1,8}I_{L1,L2}/E$ corresponds to the inductor current $I_{L1,L2}$ (parameters, see Table I).

The piecewise linear function $f(V_{C1,C3})$ has a slope $a_{1,2}$ in the inner region near the equilibrium at the origin and a slope $b_{1,2}$ in the outer regions close to the two mirror symmetric equilibria[26,27] of each oscillator. E denotes the saturation voltage of the op-amps approximated as $E\approx 1$. The slopes $a_{1,2}$ and $b_{1,2}$ are given in terms of circuit components by[27]

$$a_{1,2} = \left(-\frac{1}{R_{2,9}} - \frac{1}{R_{5,12}}\right)R_{1,8}, \quad b_{1,2} = \left(\frac{1}{R_{3,10}} - \frac{1}{R_{5,12}}\right)R_{1,8}. \tag{3}$$

Two similar state variables $x_1=V_{C1}$ and $x_2=V_{C3}(E\approx 1)$ of the coupled oscillators at the nodes of capacitors C_1 and C_3, respectively, are monitored using two channels of a digital oscilloscope (TEKTRONIX, TDS 220) for varying coupling resistance R_C. Data acquisition is made for 2500 data points at each snapshot by an 8-bit memory (100 MHz) of the oscilloscope. All circuit component values are precisely measured using a standard LCR-Q bridge (APLAB 4910).

For the synchronization analysis, the instantaneous phases $\phi_{1,2}(t)$ of the measured scalar signals, both in coupled and uncoupled states, are determined using the Hilbert transform.[3,7] The mean frequency $\Omega_{1,2}$ of each oscillator is estimated as the mean rate of the change in $\phi_{1,2}(t)$. A simple index of the relative frequency difference, $\Delta\Omega(\epsilon)=2(\Omega_1-\Omega_2)/(\Omega_1+\Omega_2)$, is taken as a measure of the frequency disorder.[15,19] $\Delta\Omega(\epsilon)$ describes the frequency difference as percentage of the mean frequencies of the coupled oscillators, $\Omega_i(\epsilon)$ $(i=1,2)$. Phase synchronization is established when this relative frequency difference $\Delta\Omega$ disappears $(\Delta\Omega\approx 0)$.

The natural frequencies of the oscillators $\omega_{1,2}=2\pi f_{1,2}$ in the uncoupled state are also estimated as the mean rate of change of the instantaneous phases $\phi_{1,2}(t)$ of the measured scalar signals $V_{C1,C3}(t)$ for each change in the parameter of

TABLE I. Circuit parameters.

L_1=20.3 mH	r_{01}=46.7 Ω	C_1=9.59 nF	C_2=95.6 nF	R_2=3215 Ω	R_3=21.28 kΩ	R_5=2147 Ω
$L2$=20.51 mH	r_{02}=47.4 Ω	C_3=9.93 nF	C_4=93.3 nF	R_9=3186 Ω	R_{10}=21.26 kΩ	R_{12}=2106 Ω

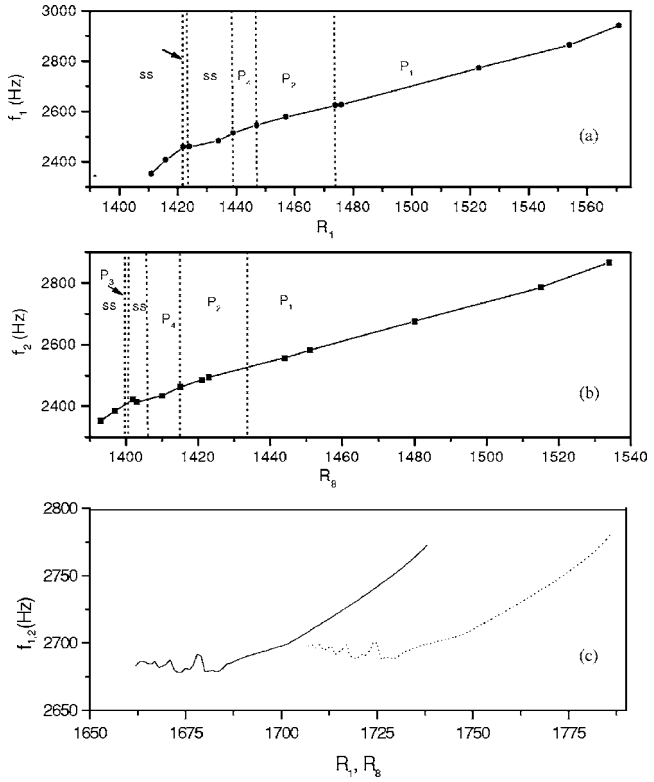

FIG. 2. Natural frequency bifurcation for the uncoupled oscillators. Experimental results for the OS-1 oscillator (a) and for OS-2 oscillator (b); the dynamical regimes are denoted as P_1 (period-1), P_2 (period-2), P_3 (period-3), P_4 (period-4) and SS (single scroll chaos). Results of numerical simulation for OS-1 (dotted line) and OS-2 (solid line) in (c). In the simulations, starting in the P_1 regime for high values of $R_{1,8}$, oscillator OS-1 undergoes a transition to P_2 at $R_1=1747$, to P_4 at $R_1=1736$, and to SS at $R_1=1732$, respectively; oscillator OS-2 undergoes a transition to P_2 at $R_8=1702$, to P_4 at $R_8=1690$, and to SS at $R_8=1680$, respectively. The frequency $f_{1,2}(=\omega_{1,2}/2\pi)$ is estimated as the mean rate of change of phase of the measured scalar signals $V_{C1,C3}(t)$ for each $R_{1,8}$ value in the uncoupled state of the oscillators.

the oscillators. As detailed in Ref. 28 the natural frequency of a single (uncoupled) Chua oscillator is a function of several circuit parameters, including the nonlinearity parameters of the oscillators, which are represented by the slopes of the piecewise linear function $\Omega_{1,2}=f(L_{1,2},C_{2,4},C_{1,3},R_{1,8},a_{1,2},b_{1,2})$. This functional dependence of the natural frequency of the oscillator on two or more control parameters is an essential criterion for APS as established in Ref. 19 in order to induce APS in coupled Rössler oscillators. Since we are interested here in the synchronization of two nonidentical oscillators and it is natural that no two similar off-the-shelf components are identical (see Table I), all the circuit components were taken to be different. In this way we introduce a mismatch in the natural frequencies of oscillations.

The Chua circuit is well known to show the limit cycle to chaotic oscillations through different routes as period-doubling or period-adding bifurcations.[26,27] Throughout this paper, all components are kept fixed except for the resistances $R_{1,8}$, which are varied to obtain the different dynamical regimes from periodic to chaotic, and also to adjust the mismatch in the natural frequencies between the two oscillators. In Figs. 2(a) and 2(b) the experimental frequency-parameter bifurcations are plotted, which are obtained by changing the resistances R_1 and R_8 of the single (uncoupled) oscillators OS-1 and OS-2, respectively. The different oscillatory windows in the frequency-parameter space are denoted as P_n $(n=1,2,3,4)$ for the period-n regime and SS for single scroll chaos. In our experiment we could only identify periodic windows up to the period-3 (P_3) window in the period-adding regime, since higher period windows in this regime were found to be very narrow.

The frequency-parameter diagram for the numerical simulation is shown in Fig. 2(c). The numerical simulations yield an excellent reproduction of the qualitative behavior that is exhibited in the experiments. Especially, by reducing the resistances $R_{1,8}$, they reproduce the same sequence of transitions from periodic windows to single scroll chaos (with very similar attractor topologies), together with a simultaneous decay of the natural frequency. However, there are some differences in the exact value of the realized frequencies. Whereas in the numerical simulations the spreading of the natural frequency is about 100 Hz from P_1 to SS, in the experiments we observe a nearly four times larger change of frequencies, of around 400 Hz. This discrepancy could have been improved in several ways by refining the simulation model, e.g., by taking into account the leakage in capacitors, by trying more realistic models of the analog devices (μ741) to improve upon the piecewise-linear modelling of the function $f(x_{1,2})$ in Eq. (2), or by estimation of an optimal parameter set that allows for the best representation of the experimental results. It may be noted that matching experiments with models is always a difficult proposition, especially in coupled chaotic oscillators.[29] This is due to several natural imperfections including noise that necessarily exists in real systems, which are difficult to model. Therefore, we set our aim here not to numerically reproduce the Chua circuit in the very best way. But instead, we chose to run the numerical simulations with exactly the same measured values of the circuit elements that have been used in our experiments (see Table I). Consequently, also in the simulations we allowed the variations in our main bifurcation parameter $R_{1,8}$. With the help of the frequency curves in Fig. 2, we were able to adjust an arbitrary natural frequency mismatch between the two oscillators in terms of the resistances R_1 and R_8, which later was used as an important control parameter.

In the experiments the induction of the PS has been performed as follows. First, fixed values of the resistances $R_{1,8}$ have been chosen in the uncoupled state (R_C is open) to achieve a desired dynamical behavior and also to select the frequency mismatch, $\Delta\omega$. Then, the interaction between the oscillators was successively introduced by decreasing the coupling resistance R_C $(=1/\epsilon)$ from 400 kΩ. For each level of coupling strength, the individual frequencies $\Omega_{1,2}(\epsilon)$ and the relative frequency difference $\Delta\Omega(\epsilon)$ were estimated from the measured time series of two coupled oscillators. In the numerical simulations, we always searched for such combinations of parameter values $R_{1,8}$ that allow for the best reproduction of the experimental results. Due to the shift in the frequency-parameter curves between experiment and simulation (see Fig. 2), this always resulted in a shift in the optimal parameter range (compared to the experimental parameter

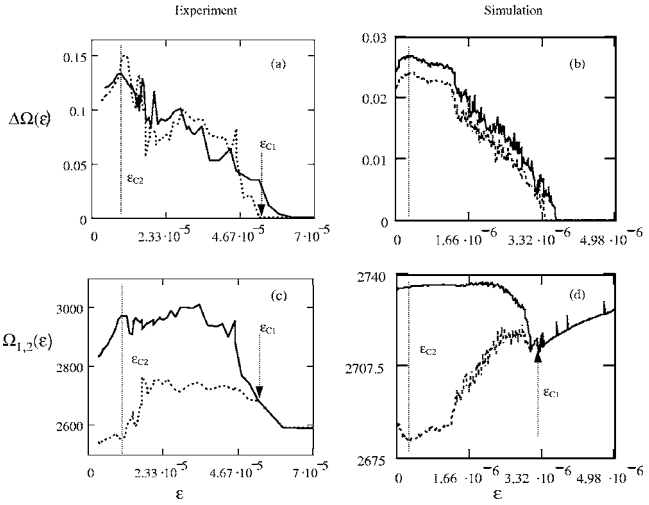

FIG. 3. Anomalous phase synchronization: frequency difference $\Delta\Omega(\epsilon)$ first increases with coupling strength, ϵ, and then decreases to in-phase synchrony. (a) Experimental results for two natural frequency mismatches, $\Delta\omega=279$ Hz (dotted line, $R_1=1570\ \Omega$ for OS-1, $R_8=1449\ \Omega$ for OS-2) and $\Delta\omega=289$ Hz (solid line, $R_1=1570\ \Omega$ for OS-1, $R_8=1447\ \Omega$ for OS-2). OS-1 and OS-2 are both parameterized in period-1. (b) Results from numerical simulations with natural frequency mismatches $\Delta\omega=47.66$ Hz (dotted line, $R_1=1765\ \Omega$, $R_8=1671\ \Omega$) and $\Delta\omega=59.44$ Hz (solid line, $R_1=1771\ \Omega$, $R_8=1671\ \Omega$) for OS-1 and OS-2 in period-1 and chaotic (single scroll chaotic) regime, respectively. Plotted also are the individual oscillator frequencies $\Omega_{1,2}(\epsilon)$ as a function of coupling. (c) Experimental results for frequency mismatch $\Delta\omega=279$ Hz [corresponding to the dotted line in (a)] and (d) numerical simulation for $\Delta\omega=47.66$ Hz [corresponding to the dotted line in (b)]. For small coupling, $\epsilon<\epsilon_{C2}$ (left of the vertical dotted line), frequencies are linearly detuned with coupling, with a slope that increases with the natural frequency, resulting in the effect of increasing frequency difference with coupling strength.

range), which best described a certain transition to synchronization in the simulations.

Further care has been taken to choose appropriate initial values. Depending on the set of parameters, a single Chua oscillator may have either a double scroll attractor or two coexisting single scroll attractors around two mirror symmetric equilibria.[26–28] In the numerical simulations we always set the coupled oscillators to either of the coexisting attractors by fixing the initial conditions. In the experiment, we reset the circuit whenever the attractor switched to the other coexisting attractor.

III. TRANSITION TO PHASE SYNCHRONIZATION IN TWO COUPLED CHUA OSCILLATORS

A. Anomalous transition to in-phase synchronization

In our first experiment we demonstrate the possibility that the two coupled Chua circuits exhibit an anomalous transition to PS (see Fig. 3). For these aims the resistances R_1 and R_8 were selected so that $R_1>R_8$ and further that the natural frequency $\omega_1=\Omega_1(\epsilon=0)$ of OS-1 is larger than the natural frequency of OS-2, $\omega_2=\Omega_2(\epsilon=0)$. The following relative frequency mismatch $\Delta\omega=\omega_1-\omega_2>0$ is defined as a positive mismatch (see Fig. 1). In the experiment [Figs. 3(a) and 3(c)] we used either the values $R_1=1570\ \Omega$, $R_8=1449\ \Omega$ with a natural frequency mismatch of $\Delta\omega=279$ Hz (solid line) or a second parameterization $R_1=1570\ \Omega$, $R_8=1447\ \Omega$ with a natural frequency mismatch of $\Delta\omega=289$ Hz (dotted line). For these parameters both oscillators are in the period-1 regime. In the numerical simulations [Figs. 3(b) and 3(d)] the best agreement to the experimental results was found for the resistances $R_1=1765\ \Omega$, $R_8=1671\ \Omega$ with a natural frequency mismatch of $\Delta\omega=47.66$ Hz (dotted line) and $R_1=1771\ \Omega$, $R_8=1671\ \Omega$ with $\Delta\omega=59.44$ Hz (solid line). In this case the first oscillator OS-1 is in the period-1 regime, whereas the second oscillator OS-2 is in a regime with single scroll chaos.

As can be clearly seen in Figs. 3(a) and 3(b) at small coupling levels, when the resistance R_C is decreased from a large initial value ($\sim 400\ \mathrm{k}\Omega$), the frequency difference $\Delta\Omega(\epsilon)$ first increases with coupling strength ϵ. At an intermediate coupling strength, $\epsilon=\epsilon_{C2}$, the frequency difference nearly attains a maximal value. Only for stronger coupling the frequency difference is reduced before the final onset of phase synchronization ($\Delta\Omega=0$) above a critical coupling, $\epsilon>\epsilon_{C1}$. This is an in-phase state when $|\Delta\phi|\approx 0$. In the numerical simulations, APS is not as strong as compared to the experiment. Nevertheless, its presence is quite evident from the plot of $\Delta\Omega(\epsilon)$ as a function of coupling in Fig. 3(b). Evidently, the frequency difference begins to grow without any threshold as can be seen from the two traces (solid and dotted lines) for two different values of natural frequency mismatch, $\Delta\omega$. Furthermore, for the two parametrizations we observe a shift in the critical coupling ϵ_{C1}, which is needed to attain phase synchronization. We find in Figs. 3(a) and 3(b) that the coupling threshold to synchronization increases with the natural frequency mismatch.

The individual frequencies $\Omega_{1,2}(\epsilon)$ as a function of coupling strength are shown in Figs. 3(c) and 3(d) [for one choice of the mismatch corresponding to the dotted line in Figs. 3(a) and 3(b)]. Clearly, in the range of small coupling to the left of the vertical dotted line ($\epsilon<\epsilon_{C2}$), the frequencies are linearly detuned with coupling. The slope of the detuning of the "faster" oscillator OS-1 (solid line) defined as $d\Omega_1/d\epsilon$ is larger than that of the "slower" oscillator OS-2 (dotted line), $d\Omega_2/d\epsilon$. Thus, the slope of the detuning increases with the natural frequency. This difference in the amount of detuning results in the net effect of increasing frequency difference with coupling strength. In Ref. 19 a sufficient condition for APS is defined as $d\kappa/d\omega>0$ where κ is the slope of the individual frequency detuning with coupling. This condition is clearly satisfied in our experiment during the initial rising phase of $\Omega_{1,2}(\epsilon)$ for coupling $\epsilon<\epsilon_{C2}$, and thus confirms the existence of an anomalous transition to PS in our first experiment.

B. Enhanced transition to antiphase synchronization

In our next experiment we explore a different set of system parameters where OS-1 is still faster than OS-2 ($\Delta\omega>0$), but for a smaller absolute value of the frequency mismatch and weaker coupling. In this parameter range we observe an enhanced transition to antiphase synchronization (see Fig. 4). The enhanced transition is characterized by a fast monotonic decrease of the frequency difference $\Delta\Omega(\epsilon)$ with coupling, and phase synchronization ($\Delta\Omega=0$) sets in at a smaller coupling strength $\epsilon\geqslant\epsilon_{C3}$. In fact, for $\epsilon\geqslant\epsilon_{C3}$, im-

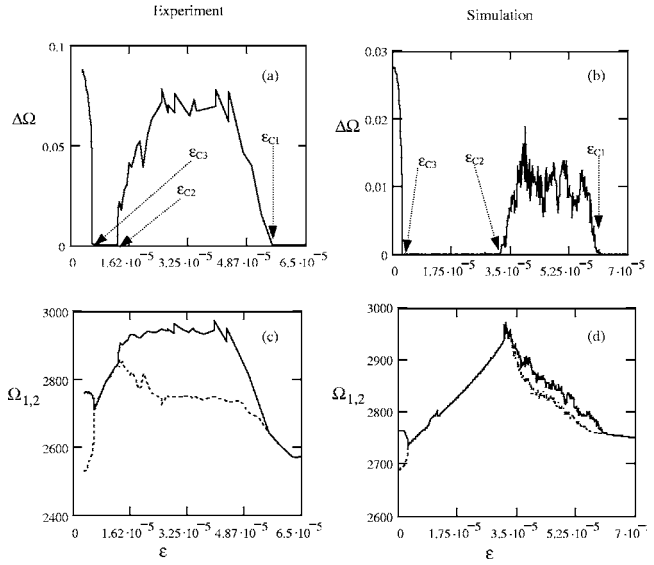

FIG. 4. Antiphase to in-phase transition for reduced frequency mismatch. Plotted are the frequency difference $\Delta\Omega(\epsilon)$ (top row) and the individual frequencies $\Omega_{1,2}(\epsilon)$ (bottom row) as a function of coupling ϵ for the experiment (left) and simulation (right). In the experiment the oscillators OS-1 and OS-2 are parameterized in the period-1 regime with parameter values $R_1=1552\ \Omega$, $R_8=1447\ \Omega$, resulting in a frequency mismatch of $\Delta\omega=239$ Hz. In the simulation OS-1 and OS-2 are in the period-1 and period-2 regime with parameters $R_1=1780\ \Omega$, $R_8=1690\ \Omega$, respectively, with a frequency mismatch of $\Delta\omega=75.39$ Hz. The two oscillators show an enhanced transition to out-of-phase synchronization ($0<\Delta\phi<\pi$) for coupling $\epsilon=\epsilon_{C3}$, and antiphase synchronization ($\Delta\phi=\pi$) for $\epsilon<\epsilon_{C2}$ just before the onset of large desynchronization in the range $\epsilon_{C2}<\epsilon<\epsilon_{C1}$, and finally in-phase synchronization ($\Delta\phi=0$) for large coupling strength $\epsilon>\epsilon_{C1}$.

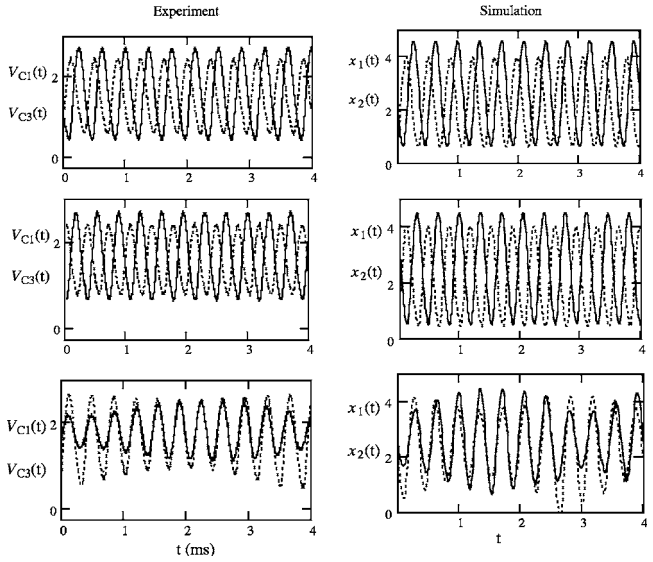

FIG. 5. Time series representing the different synchronization regimes corresponding to Fig. 4. Left column: typical experimental time series of the voltages $V_{C1}(t)$ (solid line) and $V_{C3}(t)$ (dotted line) of oscillator OS-1 and OS-2, respectively. Right column: similar numerical time series of $x_1(t)=V_{C1}(t)/E$ (bold line) and $x_2(t)=V_{C3}(t)/E$ (dotted line), $E\approx 1$. Different rows show synchronization regimes for increasing coupling strength from top to bottom. Top row: out-of-phase synchronization for coupling just after the first onset of phase synchronization $\epsilon>\epsilon_{C3}$; middle row: antiphase synchronization for coupling $\epsilon<\epsilon_{C2}$; bottom row: in-phase synchronization for large coupling values after the second onset of phase synchronization $\epsilon>\epsilon_{C1}$. Parameter values, left column: $\epsilon=5.95E-6$ (top), $\epsilon=1.28E-5$ (middle), $\epsilon=5.55E-5$ (bottom); right column: $\epsilon=3E-6$ (top), $\epsilon=2E-5$ (middle), $\epsilon=7E-5$ (bottom). Parameters otherwise as in Fig. 4.

mediately after the onset of synchronization, we observe a state of out-of-phase synchronization, which is characterized by a finite phase lag, $0<|\Delta\phi|<\pi$, between the oscillators (see Fig. 5, top row). This state gradually moves to full antiphase synchronization, $|\Delta\phi|\approx\pi$ (see Fig. 5, middle row) with increasing coupling strength, just before the onset of a second large desynchronization regime at $\epsilon\geqslant\epsilon_{C2}$. Finally, for large coupling $\epsilon\geqslant\epsilon_{C1}$, the two oscillators are again synchronized to in-phase. This second, large coupling synchronization regime for $\epsilon\geqslant\epsilon_{C1}$, however, differs from the first small coupling regime $\epsilon_{C3}<\epsilon<\epsilon_{C2}$, in the phase relation between the two locked oscillators. Instead of anti or out-of-phase synchronization, for large coupling $\epsilon\geqslant\epsilon_{C1}$, we observe a state of in-phase synchronization in which the phase lag between the two oscillators disappears, $|\Delta\phi|\approx 0$ (even though the amplitudes are not fully correlated, see Fig. 5, bottom row).

The plot of the individual frequencies $\Omega_{1,2}(\epsilon)$ as a function of coupling in Figs. 4(c) and 4(d) shows that in the range, $\epsilon<\epsilon_{C3}$, before the first transition to synchronization, the oscillator with the larger frequency is less influenced by coupling. In this range, during the transition from nonsynchronization to out-of-phase synchronization, the slopes of the individual frequencies ($d\Omega/d\epsilon$) violate the sufficient condition of $d\kappa/d\omega>0$ for APS, thus confirming again the finding of enhanced synchronization. In the antiphase synchronized state, $\epsilon_{C3}<\epsilon<\epsilon_{C2}$, the individual frequencies increase with coupling until they bifurcate again at the critical coupling $\epsilon\geqslant\epsilon_{C2}$ with the onset of a region of large desynchronization. In this intermediate coupling regime, $\epsilon_{C2}\leqslant\epsilon<\epsilon_{C1}$, we observe a phase of coexisting antiphase and in-phase states, with several topological changes in the attractor. Finally, in the in-phase synchronization regime for coupling $\epsilon\geqslant\epsilon_{C1}$, the individual frequencies show a decreasing trend as a function of coupling.

Again, our numerical results, by simulating the two coupled Chua oscillators Eq. (1) in the corresponding parameter range, perfectly agree with the experiments [see Figs. 4(b) and 4(d)]. The two oscillators show an enhanced transition to out-of-phase synchronization ($0<|\Delta\phi|<\pi$) for small coupling strength $\epsilon\geqslant\epsilon_{C3}$, antiphase synchronization ($|\Delta\phi|\approx\pi$) in the intermediate range of $\epsilon<\epsilon_{C2}$ just before the onset of the large desynchronization area, $\epsilon_{C2}<\epsilon<\epsilon_{C1}$, and finally in-phase synchronization ($|\Delta\phi|\approx 0$) sets in for large coupling strength $\epsilon>\epsilon_{C1}$.

The different synchronization states in this second experiment are visualized in Fig. 5, which depicts typical time series of either experimental results $V_{C1}(t)$ and $V_{C3}(t)$, or the numerical simulation of the similar circuit nodes of the oscillators OS-1 and OS-2.

C. Anomalous transition to antiphase synchronization

In our last experiment, we investigate the case that the uncoupled oscillator OS-2 rotates faster than OS-1, i.e., $\Omega_1(0)<\Omega_2(0)$. By reversing the sign of the natural frequency mismatch in this way ($\Delta\omega<0$), we observe an anomalous transition to antiphase synchronization as shown

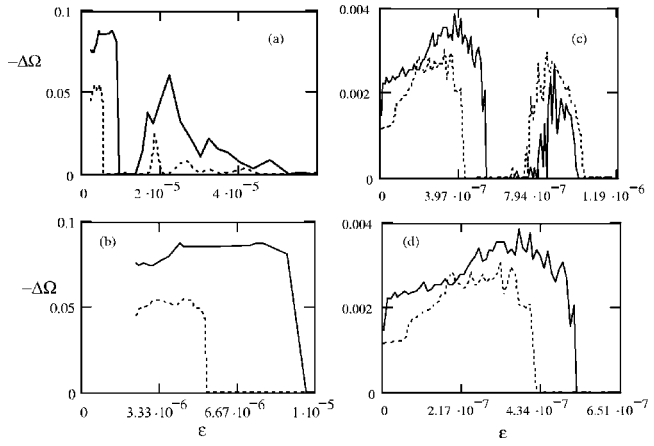

FIG. 6. Anomalous transition to antiphase synchronization for an inverted natural frequency mismatch. Plotted is the negative frequency difference, $-\Delta\Omega(\epsilon)$, as a function of coupling ϵ. The oscillators are parameterized so that the natural frequencies are inverted, $\omega_1 < \omega_2$, for two different values of the frequency mismatch. Experimental results (left column): $\Delta\omega = -130$ Hz with $R_1 = 1503\ \Omega$, $R_8 = 1552\ \Omega$ (dotted lines) and $\Delta\omega = -179$ Hz with $R_1 = 1478\ \Omega$, $R_8 = 1537\ \Omega$ (solid lines). Both oscillators are in the period-1 regime. In the simulation OS-1 is in the single scroll chaos and OS-2 in the period-1 regime (right column) with parameters: $\Delta\omega = -48$ Hz with $R_1 = 1725\ \Omega$, $R_8 = 1704.5\ \Omega$ (dotted lines) and $\Delta\omega = -58$ Hz with $R_1 = 1724.5\ \Omega$, $R_8 = 1704.5\ \Omega$ (solid lines). The anomalous increase in frequency difference is visible in the magnified plot showing the small coupling region (bottom row).

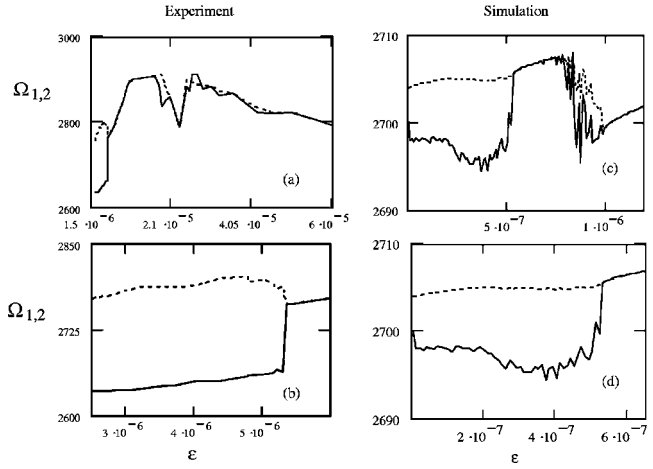

FIG. 7. Individual frequencies $\Omega_{1,2}(\epsilon)$ as a function of coupling strength ϵ in the experiments with inverted natural frequency (see Fig. 6). Left column: experimental results for the mismatch $\Delta\omega = -130$ Hz (dotted curve in Fig. 6). The necessary condition for the APS as elaborated in the text is satisfied for $\epsilon < 5E-6$. Right column: similar numerical results for $\Delta\omega = -58$ Hz (dotted curve in Fig. 6). Bottom row: magnified plot showing an enlargement of the small coupling region.

in Fig. 6. In the experiment [Figs. 6(a) and 6(b)] we use two parameter combinations with $R_1 < R_8$: first, the values $R_1 = 1503\ \Omega$, $R_8 = 1552\ \Omega$ with a natural frequency mismatch of $\Delta\omega = -130$ Hz (dotted line), and second, $R_1 = 1478\ \Omega$, $R_8 = 1537\ \Omega$ with a natural frequency mismatch of $\Delta\omega = -179$ Hz (solid line). For these parameters both oscillators are in the period-1 regime. In the numerical simulations [Figs. 6(c) and 6(d)] we use the resistances $R_1 = 1725\ \Omega$, $R_8 = 1704.5\ \Omega$ with a natural frequency mismatch of $\Delta\omega = -48$ Hz (dotted line) and $R_1 = 1724.5\ \Omega$, $R_8 = 1704.5\ \Omega$ with $\Delta\omega = -58$ Hz (solid line). In this case the first oscillator OS-1 is in a regime with single scroll chaos, whereas the second oscillator OS-2 is in period-1.

As is clearly visible in the magnified view in Figs. 6(b) and 6(d) with the onset of coupling, the two oscillators show an anomalous enlargement of their frequency difference. With further increase of coupling, the frequency difference rapidly drops down and the system approaches the first regime of phase synchronization ($\Delta\omega = 0$). An inspection of the time series reveals that in this regime the oscillators are synchronized in antiphase. In this transition to antiphase synchronization for a larger natural frequency mismatch, a larger coupling threshold is necessary to achieve synchronization [compare Figs. 6(b) and 6(d), solid lines versus dotted lines]. The out-of-phase and antiphase synchronization as discussed above are also observed for both frequency mismatches. Similar to Fig. 4 also in this experiment the first synchronization regime is intersected by the intermediate desynchronization region, characterized by large fluctuations in frequency disorder. Finally, at the high coupling end, again a second regime with in-phase synchronization is observed. The numerical results also verify the anomalous transition to antiphase for two different frequency mismatches as shown in Figs. 6(c) and 6(d). However, whereas in the experiment the second large coupling regime is an in- phase state, in the simulations in this regime the oscillators are found to be in antiphase synchronization.

The individual frequencies $\Omega_{1,2}(\epsilon)$ versus coupling are shown in Fig. 7 for both experiment and numerical simulations. Similar to the anomalous synchronization in Fig. 3, during the anomalous transition to antiphase, the magnitude of the frequency detuning (i.e., the slope of frequency change with coupling) increases with the individual oscillator frequency.

In summary, the transition to synchronization in this last experiment by reversing the sign of $\Delta\omega$ is very similar to that exhibited in Fig. 4. The major difference is that in Fig. 6 the first onset of antiphase synchronization is anomalous, whereas in Fig. 4 this first transition is enhanced.

IV. CONCLUSION

Electronic circuits have a long history as experimental systems to study phenomena in nonlinear dynamics. Especially Chua oscillators have frequently been used as one of the simplest systems for the experimental realization of chaotic dynamics and synchronization phenomena.[30] In this paper the first experimental evidence of anomalous phase synchronization is reported in two diffusively coupled Chua oscillators. So far anomalous transitions to phase synchronization have only been observed for the case of in-phase synchronization in a model system.[19] In this paper, most notably, we find an anomalous transition to antiphase both in the experiment and in the numerical simulation. We also find several other routes to synchronization, involving sequences of various synchronization states (in-phase, out-of-phase, and antiphase synchronization), which are intersected by desynchronization regimes. To the best of our knowledge these findings have not been reported earlier.

Of special interest is the desynchronization regime for intermediate coupling $\epsilon_{C2} \leqslant \epsilon < \epsilon_{C1}$ during the transition from antiphase to in-phase, where a phase of coexisting antiphase and in-phase states with large fluctuations in the frequency difference is found, together with several topological changes in the attractor. This is in contrast to the anomalous transition to PS, where the attractor topology of the oscillators changes very smoothly. The existence of an intermediate desynchronization regime with coexisting antiphase and in-phase states has recently been reported in other systems.[24,25] A coupling threshold is seen for the onset of this large desynchronization. However, no decisive statement can be made, at this point, regarding the nature of the shift in the coupling threshold, which requires more rigorous investigations.

We have shown that the nature of the transition to PS (anomalous or enhanced) depends on the sign of the natural frequency mismatch, i.e., whether $\Delta\omega$ is positive or negative. In principle, the sign of the mismatch should be arbitrary for two diffusively coupled oscillators. Nevertheless we can change the transition to PS from an anomalous to a usual (or even enhanced) transition by reversing the sign of $\Delta\omega$, using R_1 and R_8 as control parameters. We are thus able to control the synchronization in two coupled Chua circuits, either to enhance or to inhibit synchrony. Further, by controlling the sign and amount of the frequency mismatch, we are able to adjust the in-phase state into an antiphase state. All this reflects the relevance of the asymmetry of coupling, which plays a key role in the anomalous transition to phase synchronization.[20] Further experiments on the effect of coupling asymmetry will be attempted in our future work. Furthermore, our results open the door for strategies of synchronization control. With appropriate selection of system parameters, the effect of APS may be used either to enhance or to inhibit PS.

ACKNOWLEDGMENTS

S.K.D. is supported by BRNS/DAE Grant No. 2000/34/13-BRNS. B.B. is supported by the German VW-Stiftung and J.K. by DFG Grant No. SFB 555. S.K.D. wishes to acknowledge the support and hospitality extended by the Institute of Physics, Potsdam University, Germany during his two brief stays in Potsdam. J.K. acknowledges the support of the Humboldt Foundation and CSIR, India, by the Reciprocity Research Award.

[1] A. T. Winfree, *The Geometry of Biological Time* (Springer, New York, 1980).
[2] Y. Kuramoto, *Chemical Oscillations, Waves and Turbulence* (Springer-Verlag, Berlin, 1984).
[3] A. Pikovsky, M. Rosenblum, and J. Kurths, *Synchronization—A Unified Approach to Nonlinear Science* (CUP, Cambridge, 2001).
[4] J. Kurths, S. Boccaletti, C. Grebogi, and C. H. Lai, Chaos **13**, 126 (2003).
[5] H. Fujisaka and T. Yamada, Prog. Theor. Phys. **69**, 32 (1983); L. M. Pecora and T. L. Carroll, Phys. Rev. Lett. **64**, 821 (1990).
[6] N. F. Rulkov, M. M. Sushchik, L. S. Tsimring, and H. D. I. Abarbanel, Phys. Rev. E **51**, 980 (1995); L. Kocarev and U. Parlitz, Phys. Rev. Lett. **76**, 1816 (1996).
[7] A. S. Pikovsky, M. G. Rosenblum, and J. Kurths, Europhys. Lett. **34**, 165 (1996); M. G. Rosenblum, A. S. Pikovsky, and J. Kurths, Phys. Rev. Lett. **76**, 1804 (1996).
[8] S. Boccaletti, J. Kurths, G. Osipov, D. L. Valladares, and C. S. Zhou, Phys. Rep. **366**, 1 (2002).
[9] V. S. Anischenko and T. E. Vadivasova, Radiotekh. Elektron. (Moscow) **47**, 133 (2002).
[10] S. Boccaletti, E. Allaria, R. Meucci, and F. T. Arecchi, Phys. Rev. Lett. **89**, 194101 (2002).
[11] U. Parlitz, L. Junge, W. Lauterborn, and L. Kocarev, Phys. Rev. E **54**, 2115 (1996); T. L. Carroll, *ibid.* **64**, 015201 (2001); P. K. Roy, S. Chakraborty, and S. K. Dana, Chaos **13**, 342 (2003).
[12] C. Schäfer, M. G. Rosenblum, J. Kurths, and H.-H. Abel, Nature (London) **392**, 239 (1998).
[13] V. Makarenko and R. Llinás, Proc. Natl. Acad. Sci. U.S.A. **95**, 15747 (1998); P. Tass, M. G. Rosenblum, J. Weule, J. Kurths, A. S. Pikovsky, J. Volkmann, A. Schnitzler, and H.-J. Freund, Phys. Rev. Lett. **81**, 3291 (1998).
[14] J. Bhattacharya and H. Petsche, Phys. Rev. E **64**, 012902 (2001).
[15] B. Blasius, A. Huppert, and L. Stone, Nature (London) **399**, 354 (1999); B. Blasius and L. Stone, Int. J. Bifurcation Chaos Appl. Sci. Eng. **10**, 2361 (2000).
[16] K. Bar-Eli, Physica D **14**, 242 (1985); P. C. Matthews and S. H. Strogatz, Phys. Rev. Lett. **65**, 1701 (1990).
[17] S. K. Han, C. Kurrer, and Y. Kuramoto, Phys. Rev. Lett. **75**, 3190 (1995).
[18] J. F. Heagy, L. M. Pecora, and T. L Carroll, Phys. Rev. Lett. **74**, 4185 (1994); L. M. Pecora, Phys. Rev. E **58**, 347 (1998).
[19] E. Montbrió and B. Blasius, Chaos **13**, 291 (2003); B. Blasius, E. Montbrió, and J. Kurths, Phys. Rev. E **67**, 035204 (2003).
[20] B. Blasius, Phys. Rev. E **72**, 066216 (2005).
[21] J. Bragard, S. Boccaletti, and H. Mancini, Phys. Rev. Lett. **91**, 064103 (2003); J. Bragard, E. Montbrió, C. Mendoza, S. Boccaletti, and B. Blasius, Phys. Rev. E **71**, 025201 (2005).
[22] D. G. Aronson, G. B. Ermentrout, and N. Kopell, Physica D **41**, 403 (1990).
[23] D. E. Potsnov, S. K. Han, O. V. Sosnovtseva, and C. S. Kim, J. Diff. Eqns. **10**, 115 (2002).
[24] O. Popovych, V. Krachkovskyi, and P. A. Tass, in Proceeding of the NDES 2003 (2003), Vol. 197.
[25] D. He and L. Stone, Proc. R. Soc. London, Ser. B **270**, 1519 (2003).
[26] L. O. Chua, M. Komuro, and T. Matsumoto, IEEE Circuits Syst. Mag. **33**, 1073 (1986).
[27] M. P. Kennedy, IEEE Trans. Circuits Syst., I: Fundam. Theory Appl. **40**, 657 (1993).
[28] A. S. Elwakil and M. P. Kennedy, IEEE Trans. Circuits Syst., I: Fundam. Theory Appl. **47**, 76 (2000).
[29] Y-C. Lai, C. Grebogi, Phys. Rev. Lett. **82**, 4803 (1999).
[30] L. Pecora and T. Carroll, *Nonlinear Dynamics in Circuits* (World Scientific, Singapore, 1995).